

Computer Animation of the Walking Mechanics of *Australopithecus sediba*

AMEY Y. ZHANG

DALI Lab, Dartmouth College, Hanover, NH 03755, USA; zhang.amy.yun@gmail.com

JEREMY M. DESILVA

Department of Anthropology, Dartmouth College, Hanover, NH 03755, USA; and, Evolutionary Studies Institute, University of the Witwatersrand, Private Bag 3, Wits 2050, Johannesburg, SOUTH AFRICA; jeremy.m.desilva@dartmouth.edu

submitted: 29 September 2017; accepted 23 July 2018

ABSTRACT

Bipedal locomotion is one of the defining features of hominins—the lineage consisting of human ancestors and extinct relatives. Fossilized bones of the foot, leg, and pelvis, together with preserved footprints, demonstrate that the early hominin genus *Australopithecus* was an obligate biped. However, recent fossil discoveries indicate that there was bipedal diversity in *Australopithecus*, with different species walking in biomechanically distinct ways. One such hominin, *Australopithecus sediba*—a nearly 2 million-year-old species discovered in South Africa in 2008—possessed anatomies of the foot, ankle, knee, and pelvis that are consistent with a hyperpronatory gait. Though this hypothesis was published in 2013, it has remained a difficult bipedal motion to visualize and communicate to colleagues and the general public alike. Using a 3D surface scan of the partial skeleton of *Au. sediba* as a template and rigging the model in Autodesk Maya, a digital animation of the proposed walking mechanics in this ancient human relative is presented here. It is partially from this visualized form of walking that predictions can be generated to continue to test the hyperpronation hypothesis.

This special issue is guest-edited by Jeremy M. DeSilva (Department of Anthropology, Dartmouth College) and Scott A. Williams (Department of Anthropology, New York University). This is article #9 of 9.

INTRODUCTION

It is well established that upright walking evolved in the human lineage by at least 4 million years ago (Leakey et al. 1995), and it may go back even more distant in time (i.e., Brunet et al. 2002). The 3.66 million-year-old Laetoli footprints were made by an upright walking hominin (Day et al. 1980), presumably members of the same species—*Australopithecus afarensis*—best represented by the famous “Lucy” skeleton. These footprints, the Lucy partial skeleton, and dozens of isolated fossils from the lower limb of *Australopithecus* demonstrate that early members of this genus locomoted in a fully bipedal manner (Lovejoy 1988). While debates focused on whether *Australopithecus* also climbed trees and whether their mechanics of bipedalism were more (e.g., Latimer and Lovejoy 1990) or less (e.g., Stern and Susman 1983) human-like, few scholars suggested anything but a single form of bipedalism at any one time during human evolution (but see Robinson 1972 and Harcourt-Smith and Aiello 2004 who accurately predicted differences in bipedal kinematics in different australopithecine species). This linear narrative of human bipedal evolution changed quite dramatically with the publication of two re-

cent fossil discoveries.

First, a 3.4 million-year-old partial foot from Burtele, Ethiopia possessed a grasping big-toe (Haile-Selassie et al. 2012). This fossil revealed that living contemporaneously with Lucy and her kind was yet another form of early hominin, walking with different bipedal mechanics. However, the precise nature of walking in this creature, and even its taxonomic identity (Haile-Selassie et al. 2015) remains unknown until more of its postcranial remains are discovered in association with attributable craniodental fossils. Additionally, as detailed in this volume, partial skeletons of a 1.977 Ma species of hominin called *Australopithecus sediba* (Berger et al. 2010) have been recovered from Malapa, South Africa. The two partial skeletons represent a juvenile male (known as MH1 or “Karabo”) and an adult female (MH2). The fossilized remains of this species include the craniodental anatomy (Berger et al. 2010; Irish et al. 2013; de Ruiter et al. 2018), arm (Churchill et al. 2013; Churchill et al. 2018b), hand (Kivell et al. 2011; Kivell et al. 2018), torso and back (Williams et al. 2013; Williams et al. 2018), pelvis (Kibii et al. 2011; Churchill et al. 2018a), hip and leg (DeSilva et al. 2013; DeSilva et al. 2018), and parts of the foot (Zipfel et

al. 2011; DeSilva et al. 2018). Preserved regions of the lower back, hip, knee, ankle, and foot are particularly informative for reconstructing gait mechanics in an ancestral hominin. Interestingly, in many ways these key anatomies for understanding bipedal gait are morphologically different from these same regions in other fossil hominins, including *Au. africanus* (DeSilva et al. 2013). Since the shapes of bones reveal their function, the *Au. sediba* skeletons provide some of the best evidence yet discovered that different species of *Australopithecus* walked in biomechanically different ways. Additional discoveries made in the last decade have further revealed that bipedal mechanics likely differed across species of *Homo* as well (Harcourt-Smith et al. 2016; Jungers et al. 2009; Marchi et al. 2016; Ward et al. 2015).

*Australopithecus sediba* possessed a gracile, ape-like calcaneus; strikingly more primitive than the large-robust heel found in *Au. afarensis* (Zipfel et al. 2011). The gracility of the calcaneus is in part a function of a more ape-like, dorsally placed lateral plantar process (Boyle et al. 2018; Zipfel et al. 2011), which in modern humans and in *Au. afarensis* is more plantarly positioned, increasing the volume of the heel. Unlike the foot of other known fossil hominins, the *Au. sediba* midfoot was mobile and could produce a “midtarsal break” (DeSilva et al. 2013). This midfoot mobility is present in all non-human primates (DeSilva 2010), and present in a small, but not insignificant, fraction of modern humans (DeSilva and Gill 2013; DeSilva et al. 2015). Additionally, while the ankle was human-like in many respects, *Au. sediba* had an enlarged medial malleolus, and a highly mobile subtalar joint, anatomies found in the inverted foot of climbing apes (Zipfel et al. 2011). The foot of *Au. sediba* appeared primitive in many respects (likely a function of frequent and proficient tree climbing in this hominin), but there were anatomies that were also quite derived. The distal femur possessed a human-like bicondylar angle, which positions the knees directly over the feet in a striding bipedal animal. Additionally, the distal femur possessed a high lateral lip, which acts as a barrier to keep the patella from being pulled laterally out of the patellar groove in modern humans. However, the *Au. sediba* femoral lateral lip is considerably higher than that typically found in humans today (DeSilva et al. 2013). Additionally, the lower back of *Au. sediba* was highly lordotic (Williams et al. 2013). Finally, there are two osteophytic growths at the pelvic origin of *M. rectus femoris*, and the proximal fibular insertion for *M. biceps femoris*, that may be indicative of increased rotation of the lower limb in *Au. sediba* generally, and MH2 specifically (DeSilva et al. 2013), though a relationship between entheses morphology and muscular use has been questioned (e.g., Zumwalt, 2006).

We deduced that this combination of unusual anatomies was consistent with a hyperpronatory gait in *Au. sediba* (DeSilva et al. 2013). Because it possessed a gracile calcaneus, it was hypothesized that heel-striking in a human-like manner would introduce damagingly high stress on the calcaneus of *Au. sediba*. Instead, it was proposed that *Au. sediba*'s foot landed on the outside edge of an inverted foot, similar to foot touchdown observed at times

in modern apes (Vereecke et al. 2003). However, unlike in modern apes, which achieve foot inversion at both the subtalar and talocrural joints, inversion of the foot would occur solely at the mobile subtalar joint in *Au. sediba*, given the human-like talocrural joint in this hominin (Zipfel et al. 2011). Landing on the edge of an inverted foot (at the subtalar joint, but not talocrural joint) would introduce a shearing force through the medial ankle of *Au. sediba*, and the thick medial malleolus was proposed as an adaptive response to this form of walking. Both the MH2 distal tibia and an isolated tibia from another adult MH4 (U.W. 88-21) possess unusually thick malleoli (DeSilva et al. 2013; Zipfel et al. 2011). Humans today who land on the outside edge of their foot incur a pronatory torque in which the foot is driven by ground reaction forces into rapid pronation (Holt and Hamil 1995). Stance phase pronation unlocks the ligaments of the midfoot and renders the foot highly mobile—a condition which is unusual and occasionally pathological in modern humans, but is present in *Au. sediba* as evidenced by the convex base of its fourth metatarsal (DeSilva et al. 2015), the only such convex Mt4 base found in the hominin fossil record (DeSilva et al. 2013).

Furthermore, modern human hyperpronators are at a greater risk for patellar subluxation. Elevated medial rotation of the tibia and femur in a hyperpronator increases the Q-angle and thus the lateral pull of the quadriceps muscle, which increases the likelihood of patellar dislocation (Rothbart and Estabrook 1998). *Au. sediba* appears to have evolved an anatomical solution to the very problem humans face today if they hyperpronate in possessing an exceptionally high lateral lip. However, walking in this manner is not without cost. Extreme rotation of the lower limb would strain any muscle crossing both the hip and knee joint and may have resulted in the osteophytes present at the origin of *M. rectus femoris* on the anterior inferior iliac spine of the pelvis and the insertion for *M. biceps femoris* on the proximal end of the fibula (DeSilva et al. 2013).

This hypothesis has not been without criticism, which most notably asked why such an ungainly walk would evolve at all (Kimbel 2013). We propose that this form of walking was, in part, a compensatory gait in a hominin well-adapted for a dual life on the ground and in the trees. There is evidence from the upper limb (Churchill et al. 2013; Churchill et al. 2018b; Rein et al. 2017), cervical vertebrae (Meyer et al. 2018), and from its diet (Henry et al. 2012) that *Au. sediba* was comfortable in an arboreal environment and it is likely that adaptations for surviving in an arboreal environment would impact the mechanics of terrestrial gait. In other words, there was a trade-off and the gait of *Au. sediba* was seemingly unusual precisely because it was such an arboreally-adapted hominin, perhaps more so than any other species of *Australopithecus* yet discovered.

The *Au. sediba* skeletons are not yet complete and there are key anatomies of the foot skeleton that have not yet been discovered (i.e., the hallux). The hyperpronation hypothesis is based on the anatomies currently known from the *Au. sediba* skeletons (particularly MH2) and will be reevaluated as additional material is recovered. While this hypoth-

esis has been criticized by some (Kimbel 2013), others have found additional support for this proposed mechanism of gait (Prang 2016). However, whether it has been accepted or not, the hyperpronation hypothesis appears to be consistently misunderstood. Multiple news reports described this as a “pigeon-toed” gait (Choi 2013; Innes 2013; Viegas 2013) even though the hypothesis makes no mention of the orientation of the foot relative to the tibial shaft. Hyperpronators can walk with a toe-in, or toe-out position of the foot relative to the tibia (unpublished data). Some have suggested this gait involved less medial weight transfer typical of other australopiths (Fleagle and Lieberman 2016), though the hypothesis actually calls for increased medial weight transfer. Others suggested that *Au. sediba* “swayed side-to-side” (Jurmain et al. 2017), which is unlikely given the vertical orientation of the iliac blades and human-like hip abductor mechanism (Kibii et al. 2013), though we remain open to this possibility (Ruff and Higgins 2013). One reason for these misunderstandings is the fact that it is difficult to describe gait in words and instead walking mechanics are more effectively visualized. Humans are fine-tuned to subtle gait variation and can use those cues to identify individuals (Cutting and Kozlowski 1977), their sex classification (Lee and Grimson 2002), and can even infer emotional states from gait kinematics (Roether et al. 2009). It is therefore critical for effectively communicating the hyperpronation hypothesis to colleagues and to the general public alike that these gait mechanics be digitally rendered and easily visualized.

This is not the first attempt to digitally reconstruct gait in a fossil hominin. A 3D digital animation of the A.L. 288-1 “Lucy” skeleton has been published (Nagano et al. 2005) and compared with a model of the Nariokotome *Homo erectus* skeleton (KNM-WT 15000) to infer locomotor kinematics in *Australopithecus* and early fossil *Homo* (Wang et al. 2004). Our intent in developing this model of walking in *Au. sediba* is to: A) more effectively communicate to the scientific community and the general public how the hyperpronation hypothesis predicts *Au. sediba* to have walked; B) provide a 3-dimensional model available to researchers interested in using inverse dynamics to calculate joint torques on *Au. sediba* during walking to continue to make predictions about its skeletal adaptations for this mode of walking; and C) provide a 3-dimensional model for those interested in applying forward dynamic modeling to further test, refine, or if the evidence calls for it, refute the hyperpronation hypothesis; and D) provide a methodological template by which future fossil hominin skeletons can be animated either to stimulate scientific inquiry and/or the general public’s interest in our science.

## MATERIALS AND METHODS

A 3D surface scan of the composite *Au. sediba* skeleton was produced from casts of the original fossils, articulated into a standing skeleton by P. Schmid (Figure 1). The scan was made with a Creaform Go!Scan 50 from AMETEK Ultra Precision Technologies. Using the Creaform software (VX Elements), the scans were cleaned, merged, and a mesh



Figure 1. Reconstruction of *Australopithecus sediba* in lateral view. The nearly 2 million-year-old partial skeleton from Malapa, South Africa has been articulated, scanned, and is presented in digital form in lateral view. Notice the lordotic spine and the extended hips and legs.

was created with a 2mm resolution, which was exported as an STL file. In regions of anatomical interest for bipedal gait (hip, knee, ankle, and foot), isolated casts, and in some cases original fossil material, were scanned at a higher resolution with a Creaform Go!Scan 20 scanner from AMETEK Ultra Precision Technologies. Once again, these files were cleaned, merged, and a mesh created with a 0.2mm resolution, and exported as STL files. Meshmixer was used to convert the files from STL to OBJ so that they could be opened and manipulated in Autodesk Maya 2016. Scans were aligned to a center axis.

In Autodesk Maya 2016, a new mesh was created for each bone. The mesh generated from the scanner is made up of triangles and often contains overlaps and irregularities that can complicate rendering and animation in later steps. This new mesh was made of quads and four-way intersections, with a few triangles and five-way intersections when necessary. Edges were defined by following the contours of the bone.

The surface scan was made a Live Surface. For bones that were well-defined in the scan, Quad Draw was used to draw a new mesh over the scan. The vertices of the new mesh were snapped to the Live Surface. For bones that were poorly defined in the surface scan, a modern human skeleton model or a rough, approximate shape from a basic polygon was used. The model was positioned, scaled, and sculpted to approximate the form and position of the desired bone in the scan. In the vertex mode, all vertices of the new bone were selected. The scan was made a Live Surface, and the vertices were scaled to match the mesh and adjusted as necessary.

Missing areas or detail were added first by increasing

the resolution by inserting edge loops into a specific area or by using Smooth Mesh on the entire bone. Vertices of the region of the model were selected and either scaled or moved to match the Live Surface scan. In cases where a higher resolution scan existed for a region of anatomical interest (e.g., ankle, knee), the OBJ file of that element was imported, positioned, and scaled to the appropriate location in the full scan. The new template scan was made a Live Surface and relevant vertices in the model were selected and scaled to match the Live Surface. In cases where a higher-resolution scan did not exist, Fill Hole and Multi-Cut tools were used to create and define the mesh in the missing region. Vertices were manually moved to approximate the correct geometry.

The new mesh was created for one side of the body and then reflected across the central axis using Mirror Geometry. Vertices were combined for bones on the central axis. Before rigging, the surface scan was hidden and the bones of the clean mesh were positioned to match the T-position of the rig.

The foot was rigged first. Joints of the rig were matched to the bones of the model, allowing the model to bend at that joint location. To keep the bones of the toes from pulling apart as the foot bent, the ball and toe joints of the foot were positioned between the first and second toes of the mesh. A midfoot joint was located at the lateral tarsometatarsal joint (between the cuboid and the lateral metatarsals) and medially between the second metatarsal and the intermediate cuneiform such that the foot rig had heel, midfoot, ball, and toe joints. Inverse Kinematic (IK) handles were created successively at the hip, heel, midfoot, ball, and toe joints. Controls were created for the foot, heel, midfoot and toe; the parent function was used to link toe and midfoot controls to the foot control; the heel to midfoot control; heel IK and leg IK to heel control; midfoot IK to midfoot control; and toe IK to toe control. Standard rigging best practices were used to control the rest of the body.

The model was bound to the completed rig. The bones (aside from the spine) were skinned such that they were influenced by one joint only and did not bend. The spine was skinned with multiple influences and used Paint Skin Weights to adjust the influence of each spinal joint on portions of the spine. Skin weights were tested by bending each joint to check the model's motion. The outer foot bones were skinned with influences from multiple joints to prevent them from pulling too far away from adjacent bones as the foot bent.

The model was animated using a standard human walk cycle at 32 frames/second with the following modifications. The foot strike did not start with heel contact, but rather with simultaneous contact of the lateral edge of an inverted foot. The foot then rolled medially (pronated) such that the whole foot contacted the ground. The knee medially rotated following the foot stride. The maximum rotation of the hip in the x-axis was delayed so that the forward hip continued to rotate forward past the extension position following the inward motion of the foot and knee. The back foot was animated by bending the foot at the midfoot region as



Figure 2. *Australopithecus sediba* in oblique view. Still frame from Video Figure 1. Notice the relatively long arms, and short legs (see Holliday et al. 2018) and the fully extended knee and hip. The left foot is contacting the ground in a position of slight inversion. Notice the contralateral forward motion of the right arm at this moment in the gait cycle.

the heel first lifted off the ground. As the heel continued to lift, flexion proceeded distally to the ball of the foot.

A batch render of one cycle of the animation from a camera position from the front, side, and three-quarter views was created. Each image sequence was opened in Photoshop as a video layer and exported.

## RESULTS

The hypothesized mechanics of walking in *Australopithecus sediba* are visualized by rigging and animating a 3D model based on a surface scan of the partial skeleton in Autodesk Maya. The model was created using the 3D surface scan as a template. The rig and animation are adapted from a standard human rig and walk cycle to reflect hypothesized differences in the gait of *Au. sediba* (see Holliday et al. 2018). In oblique view (Figure 2; Video Figure 1), one may notice the relatively long arms and short legs of *Au. sediba*, but walking mechanics likely appear quite modern human-like. As in modern human walking, there was likely full extension of the knee and hip in *Australopithecus* and forward motion of the leg would be counter torqued by contralateral forward motion of the arm.

In frontal view (Figure 3; Video Figure 2), notice that contact of the foot with the substrate occurs along the lateral edge of a flat and inverted foot. Because the tibia is orthogonal to the ankle joint in *Au. sediba*, as in all other hominin tibiae, inversion is occurring at the highly mobile subtalar joint, rather than the talocrural joint. As the foot



Video Figure 1. Computer animation of *Australopithecus sediba* walking in oblique view. In this view, notice the human-like walk, with an extended knee, extended hip, and little mediolateral sway during gait.

contacts the substrate, ground reaction forces drive the midfoot into excessive and rapid pronation (hyperpronation) visualized as extreme medial weight transfer. Because of the closed kinetic chain of the leg, pronation of the foot results in medial rotation of the tibia and femur as well. This motion effectively increases the Q-angle of the femur and pulls the knees toward the midline. In frontal view, medial rotation of the pelvis can be visualized as well—a motion that would effectively increase the stride length in a short-legged hominin (Rak 1991).

In lateral view (Figure 4; Video Figure 3), notice the high degree of lumbar lordosis, and full extension of the hip and knee joints during the gait cycle. Furthermore, the inverse pendular mechanics of human-like walking, in which there is an exchange of potential and kinetic energy as the center of mass rises and falls, is evident by watching the sinusoidal motion of the head. In this view, three important and unique aspects of gait in *Au. sediba* are visible. First, the foot of this hominin is flat (Prang 2015) and contacts the ground without a proper heel-strike, but with the entire lateral foot simultaneously hitting the ground. Second, as the heel lifts off the substrate, there is dorsiflexion at the lateral tarsometatarsal joint—a so-called “midtarsal break.” This motion is unusual in humans, though it can be found in modern humans that possess flat feet and a hyperpronatory gait (DeSilva et al. 2015). Finally, because it has been shown that midfoot flexibility compromises the push-off mechanism (Bates et al. 2013; DeSilva et al. 2015), the foot does not drive off the ground and instead lifts off the ground. It is likely that these mechanics of walking would reduce stride length and thus *Au. sediba* is modeled as pos-

sessing a relatively short stride length.

## DISCUSSION

This paper presents a 3-dimensional animation of the proposed mechanics of bipedal locomotion in a nearly 2-million-year-old fossil hominin species, *Australopithecus sediba*. A 3D model appropriate for animation was constructed in Autodesk Maya using a surface scan of the composite *Au. sediba* skeleton as a template. For portions of the skeleton missing in the scan, the model was approximated or filled in using other 3D surface scans of individual bones. An additional joint was inserted into a standard human rig at the midfoot, and the inverse kinematics controls on the foot were adapted to accommodate a second “break.” The animation was modified from a typical human walk cycle to illustrate the hypothesized hyperpronation gait of *Au. sediba*. The most important features include the foot strike on the outer edge of the inverted foot instead of directly on the heel, the inward rotation of the knee and hip following contact with the ground, and the midtarsal break of the midfoot during push-off (Video Figure 4).

Although the animation is based on a surface scan of an articulated *Au. sediba* skeleton, modifications to the model were made. The articulated composite skeleton possesses an anteriorly tilted torso. Lumbar lordosis was increased to bring the torso back over the hip joints, consistent with the anatomy of the MH2 skeleton (Williams et al. 2013). Some portions of the model were mirrored from the right to left side and may not possess all the asymmetries present in the articulated skeleton. The joints of the articulated composite skeleton are sealed together, and so the joints of the model

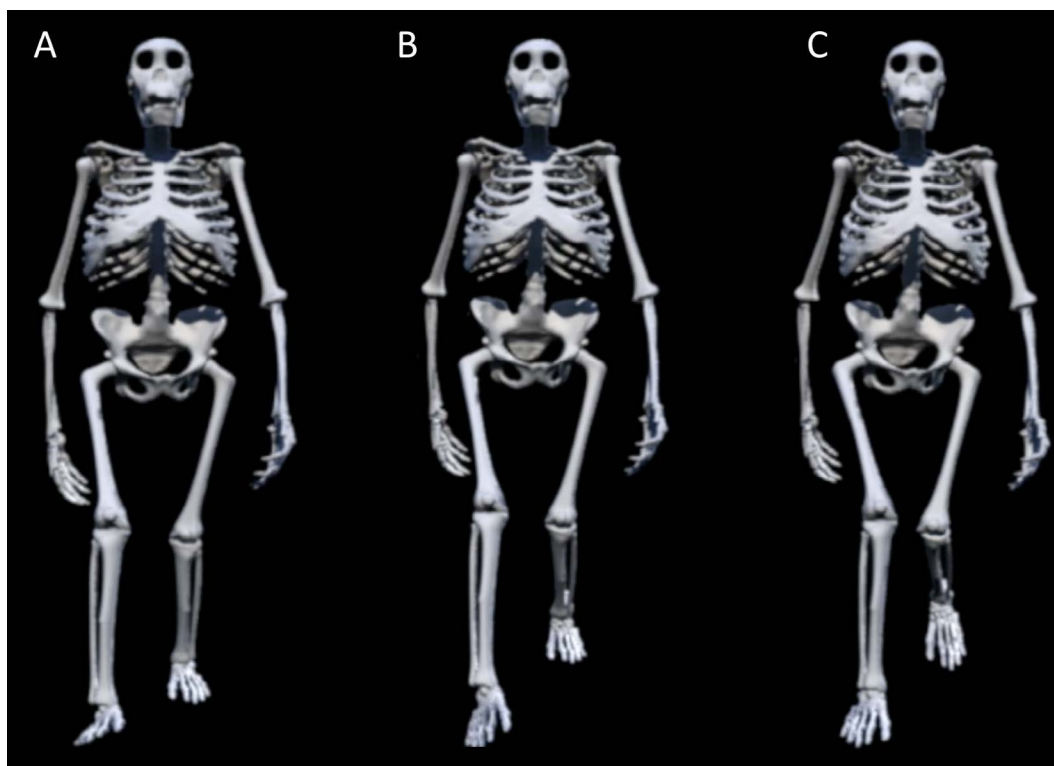
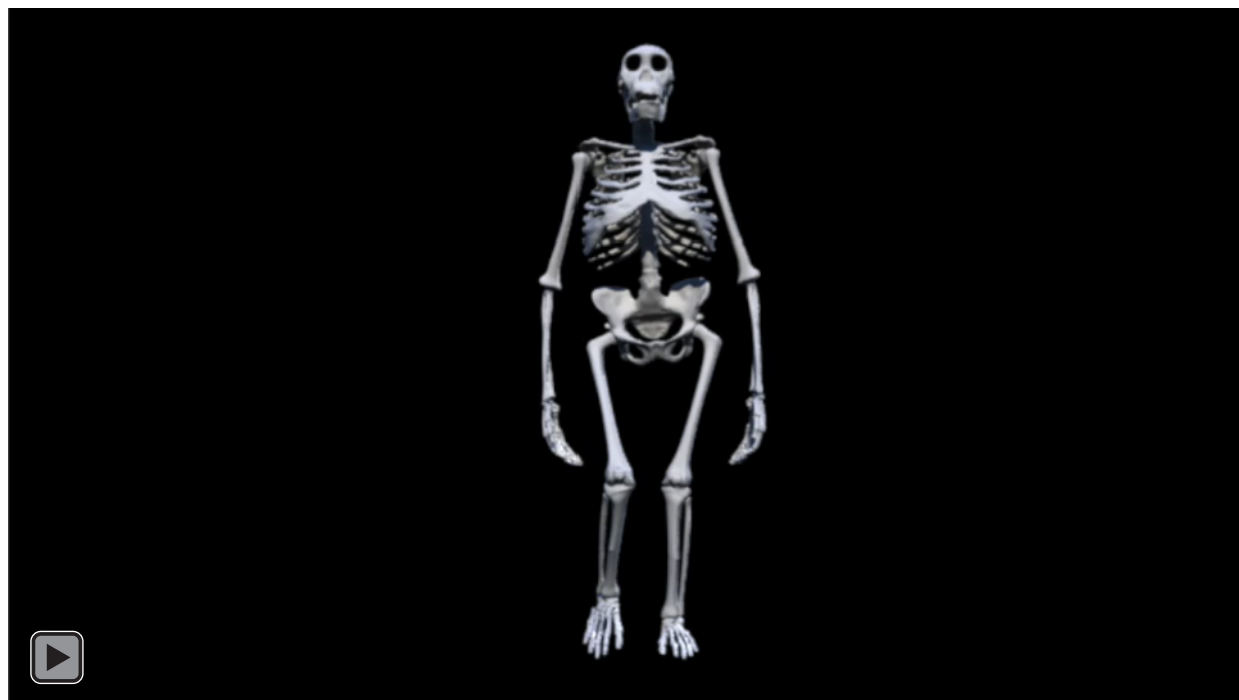


Figure 3. *Australopithecus sediba* gait in frontal view. Still frames from Video Figure 2. A) The right leg is in the final moments of swing phase. Notice that the right foot is in an inverted position—a motion occurring at the subtalar joint, but not the talocrural. B) At “heel-strike,” the foot is hypothesized to contact much of the lateral edge of the forefoot, in addition to the lateral edge of the heel. C) Foot flat is achieved rapidly as ground reaction forces drive the foot into excessive pronation (hyperpronation). This foot motion has an upstream effect, causing medial rotation of the tibia and the femur. Notice in frame “C” that the Q-angle of the femur has increased considerably from frames “A” and “B.”



Video Figure 2. Computer animation of *Australopithecus sediba* walking in frontal view. Notice the contact of the foot along the lateral edge and the rapid pronation (medial weight transfer). Notice also the medial rotation of the tibia and femur during the stance phase of gait, and the increased medial rotation of the pelvis during the swing phase.

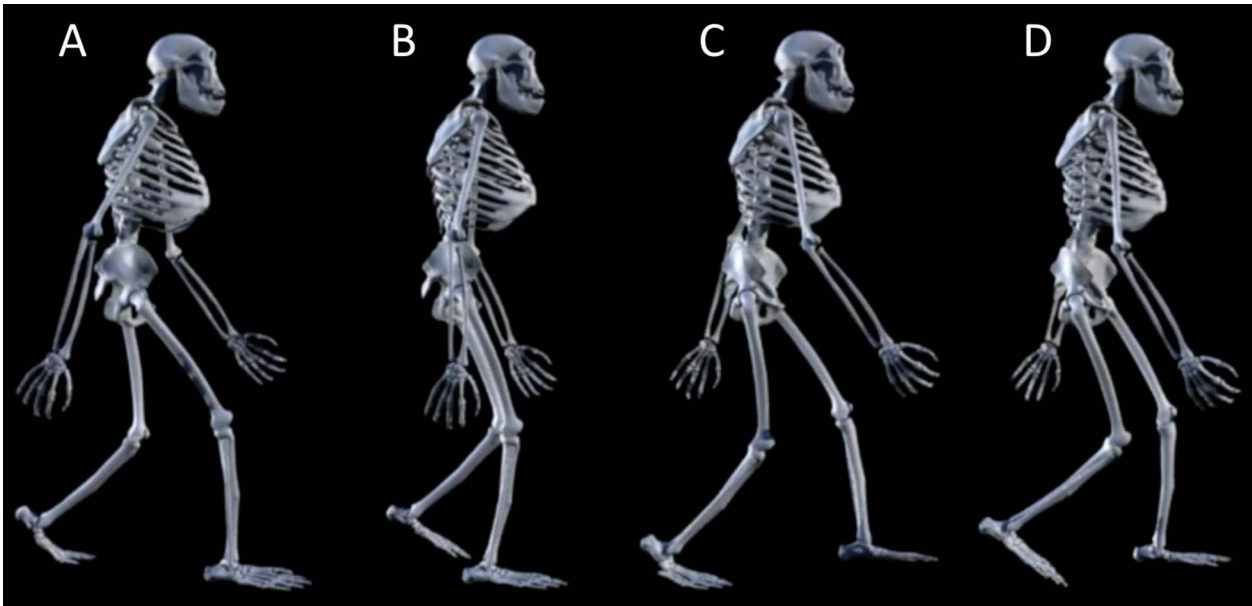


Figure 4. *Australopithecus sediba* gait in lateral view. Still frames from Video Figure 3. A) The right leg is in the final moments of swing phase; the relatively flat foot is in slight inversion. B) Right foot flat (after initial contact, the foot has fully pronated). C) Initial heel lift reveals a midtarsal break, in which dorsiflexion at the tarsometatarsal joint precedes dorsiflexion at the metatarsophalangeal joint. D) Toe-off is weak—a pronated, hypermobile foot is not able to push-off the ground as a rigid foot does (see Bates et al. 2013; DeSilva et al. 2015), resulting in shorter, less efficient strides.

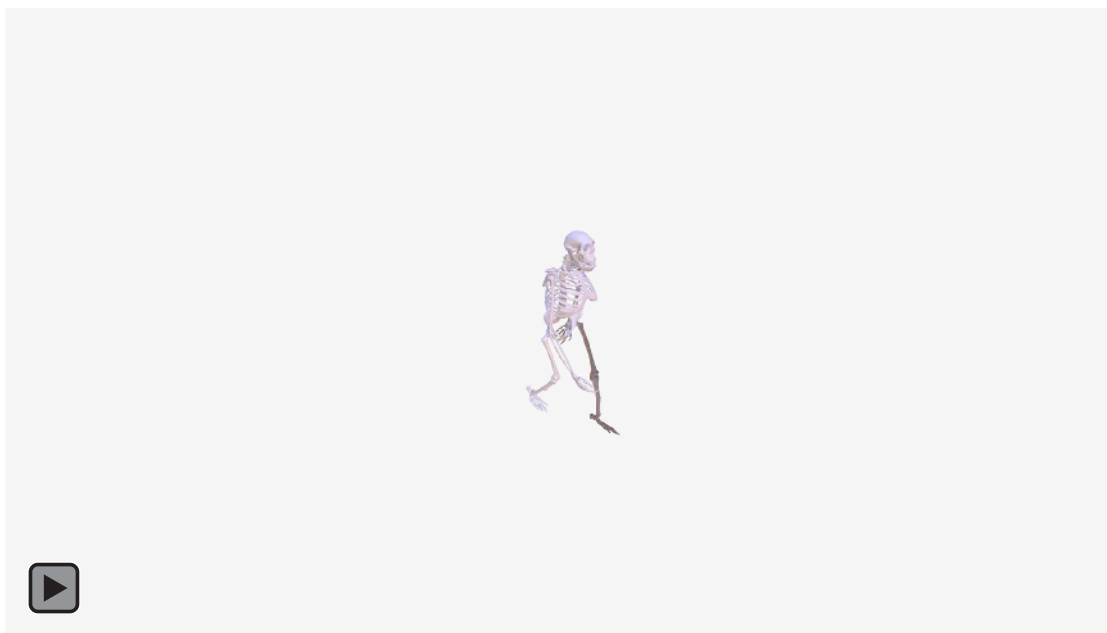
are either constructed from additional scans of individual bones or approximated. The vertices of the new model fall on the planes defined by the 3D surface scan whenever possible, but because of the reduction in number of vertices in the model and digital smoothing, the model bones may

appear narrower than the original.

Additionally, it must be recognized that although the *Au. sediba* female skeleton (MH2) is one of the more complete partial skeletons in the hominin fossil record, it is still missing a large portion of its skeleton. Some of the skel-



Video Figure 3. Computer animation of *Australopithecus sediba* walking in lateral view. Notice the flat foot and the midtarsal break occurring between the cuboid and the lateral metatarsals. In this view, the lordotic spine and fully extended hip and knee can also be visualized.



Video Figure 4. Computer animation of *Australopithecus sediba*. The animation has been set at half speed to visualize the particulars of gait described in the text (courtesy of S. Broadley).

eton was reconstructed by mirror-imaging recovered fossil anatomies. For example, the right distal femur and right arm were mirrored and replicated on the left side. Some aspects of the skeleton are known from other individuals and were used to create a composite skeleton. For example, the skull is from the MH1 individual, as is the right fourth metatarsal. Finally, there are anatomies unknown entirely for *Au. sediba* (e.g., the hallux) and are reconstructed based on what is known in general for the genus *Australopithecus*. These assumptions about the anatomy of *Au. sediba* will be reassessed should additional excavation at the Malapa cave in South Africa yield more discoveries.

Our hope is that this animation will improve general understanding of gait variation in *Australopithecus*. The 3-dimensional model is available to researchers interested in using inverse dynamics to calculate joint torques produced by *Au. sediba* during walking to continue to make predictions about its skeletal anatomy and adaptations for this mode of walking. For example, preliminary work on this skeleton from our research team using OpenSIM suggests a high moment for the adductor muscles and *M. piriiformis* in *Au. sediba*. Additionally, this 3-dimensional model is now available for those interested in applying forward dynamic modeling (as others have done with fossil hominins [Nagano et al. 2005]) to further test and refine the hyperpronation hypothesis for gait in this ancient hominin. Finally, this work presents a visual representation of a hypothesis for how an extinct human relative walked almost two million-years ago. It not only should improve both the specifics for how it is thought *Au. sediba* walked, but it should serve as inspiration and fascination for a general public eager to learn more about their evolutionary history (Pobiner 2016).

#### ACKNOWLEDGMENTS

Thank you to the University of the Witwatersrand Fossil Access Committee for approving our request to study the *Au. sediba* fossils. We are grateful to Lee Berger for his open access approach to paleoanthropology and the opportunity he has given us to study the *Au. sediba* fossil material. Peter Schmid reconstructed the articulated *Au. sediba* skeleton which formed the basis of this analysis. Thanks to colleagues Bernhard Zipfel, Ken Holt, Steve Churchill, Kristian Carlson, and Christopher Walker for their insight and important contributions during the development of the hyperpronation hypothesis. The Boston University Center for Digital Imaging Arts (CDIA) worked on a preliminary 3D animation of *Au. sediba* and we are grateful for all we learned in that process. Additionally, we are grateful to Kathleen Joseph for her work using OpenSIM on gait in *Au. sediba*. Thanks to Ellison McNutt for assistance and expertise in scanning the composite *Au. sediba* skeleton. Sawyer Broadley, and Adam Nemeroff provided feedback on the model presented here. Sawyer produced the rotating, multiple-view version of the animation (Video Figure 4). Thank you to Patricia Hannaway and James Mahoney for their guidance and feedback on modeling, rigging, and animation.

#### REFERENCES

- Bates, K.T., Collins, D., Savage, R., McClymont, J., Webster, E., Pataky, T.C., D'Aout, K., Sellers, W.I., Bennett, M.R., and Crompton, R.H. 2013. The evolution of compliance in the human lateral mid-foot. *Proceedings of the Royal Society B* 280, 20131818.
- Berger, L.R., de Ruiter, D.J., Churchill, S.E., Schmid, P., Carlson, K.J., Dirks, P.H.G.M., and Kibii, J.M. 2010.

- Australopithecus sediba*: a new species of *Homo*-like australopithec from South Africa. *Science* 328, 195–2004.
- Boyle, E.K., McNutt, E.J., Sasaki, T., Suwa, G., Zipfel, B., and DeSilva, J.M. 2018. A quantification of calcaneal lateral plantar process position with implications for bipedal locomotion in *Australopithecus*. *Journal of Human Evolution* 123, 24–34.
- Brunet, M., Guy, F., Pilbeam, D., Mackaye, H. T., Likius, A., Ahounta, D., Beauvilain, A., Blondel, C., Bocherens, H., Boissier, J.R., and De Bonis, L. 2002. A new hominid from the Upper Miocene of Chad, Central Africa. *Nature* 418, 145–151.
- Choi, C. 2013. Humanity's closest ancestor was pigeon-toed, research reveals. *LiveScience*. <https://www.livescience.com/28656-closest-human-ancestor-was-pigeon-toed.html>
- Churchill, S.E., Green, D.J., Feuerriegel, M.E., Macias, M.E., Matthews, S., Carlson, K.J., Schmid, P., and Berger, L.R. 2018b (this volume). The shoulder, arm, and forearm of *Australopithecus sediba*. *PaleoAnthropology* 2018, 234–281.
- Churchill, S.E., Holliday, T.W., Carlson, K.J., Jashashvili, T., Macias, M.E., Mathews, S., Sparling, T.L., Schmid, P., de Ruiter, D.J., and Berger, L.R. 2013. The upper limb of *Australopithecus sediba*. *Science* 340, 1233477.
- Churchill, S.E., Kibii, J.M., Schmid, P., Reed, N.D., and Berger, L.R. 2018a (this volume). The pelvis of *Australopithecus sediba*. *PaleoAnthropology* 2018, 334–356.
- Cutting, J.E. and Kozlowski, L.T. 1977. Recognizing friends by their walk: gait perception without familiarity cues. *Bulletin of the Psychonomic Society* 9, 353–356.
- Day, M.H. and Wickens, E.H. 1980. Laetoli Pliocene hominid footprints and bipedalism. *Nature* 286, 385–387.
- De Ruiter, D.J., Carlson, K.B., Brophy, J.K., Churchill, S.E., Carlson, K.J., and Berger, L.R. 2018 (this volume). The Skull of *Australopithecus sediba* (Special Issue: *Australopithecus sediba*). *PaleoAnthropology* 2018, 56–155.
- DeSilva, J.M. 2010. Revisiting the “midtarsal break”. *American Journal of Physical Anthropology* 141, 245–258.
- DeSilva, J.M., Carlson, K.J., Claxton, A., Harcourt-Smith, W.E.H., McNutt, E.J., Sylvester, A.D., Walker, C.S., Zipfel, B., Churchill, S.E., and Berger, L.R. 2018 (this volume). The anatomy of the lower limb skeleton of *Australopithecus sediba*. *PaleoAnthropology* 2018, 357–405.
- DeSilva, J.M. and Gill, S.V. 2013. Brief communication: a midtarsal (midfoot) break in the human foot. *American Journal of Physical Anthropology* 151: 495–499.
- DeSilva, J.M., Holt, K.G., Churchill, S.E., Carlson, K.J., Walker, C.S., Zipfel, B., and Berger, L.R. 2013. The lower limb and mechanics of walking in *Australopithecus sediba*. *Science* 340, 1232999.
- DeSilva, J.M., Bonne-Annee, R., Swanson, Z., Gill, C.M., Sobel, M., Uy, J., and Gill, S.V. 2015. Midtarsal break variation in modern humans: functional causes, skeletal correlates, and paleontological implications. *American Journal of Physical Anthropology* 156, 543–552.
- Fleagle, J.G. and Lieberman, D.E. 2015. Major transformations in the evolution of primate locomotion. In *Great Transformations in Vertebrate Evolution*, Dial, K.P., Shubin, N., Brainerd, E.L. (eds.). The University of Chicago Press, Chicago, pp. 257–282.
- Haile-Selassie, Y., Saylor, B.Z., Deino, A., Levin, N.E., Alene, M., and Latimer, B.M. 2012. A new hominin foot from Ethiopia shows multiple Pliocene bipedal adaptations. *Nature* 483, 565–569.
- Haile-Selassie, Y., Gibert, L., Melillo, S.M., Ryan, T.M., Alene, M., Deino, A., Levin, N.E., Scott, G., and Saylor, B.Z. 2015. New species from Ethiopia further expands Middle Pliocene hominin diversity. *Nature* 521, 483–488.
- Harcourt-Smith, W.E.H. and Aiello, L.C. 2004. Fossils, feet, and the evolution of human bipedal locomotion. *Journal of Anatomy* 204, 403–416.
- Harcourt-Smith, W.E.H., Throckmorton, Z., Congdon, K.A., Zipfel, B., Deana, A.S., Drapeau, M.S.M., Churchill, S.E., Berger, L.R., and DeSilva, J.M. 2015. The foot of *Homo naledi*. *Nature Communications* 6, 8432.
- Henry, A.G., Ungar, P.S., Passey, B.H., Sponheimer, M., Rossouw, L., Bamford, M., Sandberg, P., de Ruiter, D.J., and Berger, L.R. 2012. The diet of *Australopithecus sediba*. *Nature* 487, 90–93.
- Holliday, T.W., Churchill, S.E., Carlson, K.J., DeSilva, J.M., Schmid, P., Walker, C.S., and Berger, L.R. 2018 (this volume). Body size and proportions of *Australopithecus sediba*. *PaleoAnthropology* 2018, 406–422.
- Holt, K.G. and Hamil, J. 1995. Running injuries and treatment: a dynamic approach. In *Rehabilitation of the Foot and Ankle*, Sammarco, G.J. (ed.). Mosby, St. Louis. pp. 241–254.
- Innes, E. 2013. Pigeon-toed and unable to run: researchers shed new light on two million-year-old ‘missing link’ human ancestor. *Daily Mail*. <http://www.dailymail.co.uk/sciencetech/article-2307945/Pigeon-toed-unable-run-Researchers-shed-new-light-early-humans.html>
- Irish, J.D., Guatelli-Steinberg, D., Legge, S.S., de Ruiter, D.J., and Berger, L.R. 2013. Dental morphology and the phylogenetic “place” of *Australopithecus sediba*. *Science* 340, 1233062.
- Jungers, W.L., Harcourt-Smith, W.E.H., Wunderlich, R.E., Tocheri, M.W., Larson, S.G., Sutikna, T., Due, R.A., and Morwood, M.J. 2009. The foot of *Homo floresiensis*. *Nature* 459, 81–84.
- Jurmain, R., Kilgore, L., Trevathan, W., Ciochon, R.L., and Bartelink, E. 2017. *Introduction to Physical Anthropology*. Cengage Learning, Boston, MA.
- Kibii, J.M., Churchill, S.E., Schmid, P., Carlson, K.J., Reed, N.D., de Ruiter, D.J., and Berger, L.R. 2011. A partial pelvis of *Australopithecus sediba*. *Science* 333, 1407–1411.
- Kimbel, W.H. 2013. Paleoanthropology: hesitation on hominin history. *Nature* 497, 573–574.
- Kivell, T.L., Churchill, S.E., Kibii, J.M., Schmid, P., and Berger, L.R. 2018 (this volume). The hand of *Australopithecus sediba*. *PaleoAnthropology* 2018, 281–332.
- Kivell, T.L., Kibii, J.M., Churchill, S.E., Schmid, P., and Berger, L.R. 2011. *Australopithecus sediba* hand demonstrates mosaic evolution of locomotor and manipulative abilities. *Science* 333, 1411–1417.

- Latimer, B. and Lovejoy, C.O. 1990. Hallucal tarsometatarsal joint in *Australopithecus afarensis*. *American Journal of Physical Anthropology* 82, 125–133.
- Leakey, M.G., Feibel, C.S., McDougall, I., and Walker, A. 1995. New four-million-year-old hominid species from Kanapoi and Allia Bay, Kenya. *Nature* 376, 565–571.
- Lee, L. and Grimson, W.E. 2002. Gait analysis for recognition and classification. In *Automatic Face and Gesture Recognition*. Proceedings of the Fifth IEEE International Conference, Washington D.C. pp. 155–162.
- Lovejoy, C.O. 1988 Evolution of human walking. *Scientific American* 259, 118–125.
- Marchi, D., Walker, C.S., Pei, P., Holliday, T.W., Churchill, S.E., Berger, L.R., DeSilva, J.M. 2017. The thigh and leg of *Homo naledi*. *Journal of Human Evolution* 104, 174–204.
- Meyer, M.R., Woodward, C., Tims, A., Bastir, M. 2018. Neck function in early hominins and suspensory primates: insights from the uncinat process. *American Journal of Physical Anthropology* 166, 613–637.
- Nagano, A., Umberger, B., Marzke, M.W., and Gerritsen, K.G. 2005. Neuromuscular computer modeling and simulation of upright, straight-legged, bipedal locomotion of *Australopithecus afarensis* (AL 288-1). *American Journal of Physical Anthropology* 126, 2–13.
- Pobiner, B. 2016. Accepting, understanding, teaching, and learning (human) evolution: obstacles and opportunities. *American Journal of Physical Anthropology* 159, 232–274.
- Prang, T.C. 2015. Rearfoot posture of *Australopithecus sediba* and the evolution of the hominin longitudinal arch. *Scientific Reports* 5, 17677.
- Prang, T.C. 2016. Conarticular congruence of the hominoid subtalar joint complex with implications for joint function in Plio-Pleistocene hominins. *American Journal of Physical Anthropology* 160, 446–457.
- Rak, Y. 1991. Lucy's pelvic anatomy: its role in bipedal gait. *Journal of Human Evolution* 20, 283–300.
- Rein, T.R., Harrison, T., Carlson, K.J., and Harvati, K. 2017. Adaptation to suspensory locomotion in *Australopithecus sediba*. *Journal of Human Evolution* 104, 1–12.
- Robinson, J.T. 1972. *Early Hominid Posture and Locomotion*. University of Chicago Press, Chicago.
- Roether, C.L., Omlor, L., Christensen, A., and Giese, M.A. 2009. Critical features for the perception of emotion from gait. *Journal of Vision* 9, 15.
- Rothbart, B.A. and Estabrook, L. 1988. Excessive pronation: a major biomechanical determinant in the development of chondromalacia and pelvic lists. *Journal of Manipulative and Physiological Therapy* 11, 373–379.
- Ruff, C.B. and Higgins, R. 2013. Femoral neck structure and function in early hominins. *American Journal of Physical Anthropology* 150, 512–525.
- Stern Jr, J. T. and Susman, R. L. 1983. The locomotor anatomy of *Australopithecus afarensis*. *American Journal of Physical Anthropology* 60, 279–317.
- Vereecke, E., D'Août, K., De Clercq, D., Van Elsacker, L., and Aerts, P. 2003. Dynamic plantar pressure distribution during terrestrial locomotion of bonobos (*Pan paniscus*). *American Journal of Physical Anthropology* 120, 373–383.
- Viegas, J. 2013. Ancient ancestor had chimp and human traits. *ABC Science*. <http://www.abc.net.au/science/articles/2013/04/12/3734941.htm>
- Wang, W., Crompton, R.H., Carey, T.S., Günther, M.M., Li, Y., Savage, R., and Sellers, W.I. 2004. Comparison of inverse-dynamics musculoskeletal models of AL 288-1 *Australopithecus afarensis* and KNM-WT 15000 *Homo ergaster* to modern humans, with implications for the evolution of bipedalism. *Journal of Human Evolution* 47, 453–478.
- Ward, C.V., Feibel, C.S., Hammond, A.S., Leakey, L.N., Moffett, E.A., Plavcan, J.M., Skinner, M.M., Spoor, F., and Leakey, M.G. 2015. Associated ilium and femur from Koobi Fora, Kenya, and postcranial diversity in early *Homo*. *Journal of Human Evolution* 81, 48–67.
- Williams, S.A., Meyer, M.R., Nalla, S., García-Martínez, D., Nalley, T.K., Eyre, J., Prang, T.C., Bastir, M., Schmid, P., Churchill, S.E., and Berger, L.R. 2018 (this volume). The vertebrae, ribs, and sternum of *Australopithecus sediba*. *PaleoAnthropology* 2018, 156–233.
- Williams, S.A., Ostrofsky, K.R., Frater, N., Churchill, S.E., Schmid, P., and Berger, L.R. 2013. The vertebral column of *Australopithecus sediba*. *Science* 340, 1232996.
- Zipfel, B., DeSilva, J.M., Kidd, R.S., Carlson, K.J., Churchill, S.E., and Berger, L.R. 2011. The foot and ankle of *Australopithecus sediba*. *Science* 333, 1417–1420.
- Zumwalt, A. 2006. The effect of endurance exercise on the morphology of muscle attachment sites. *Journal of Experimental Biology* 209, 444–454.